

A Mathematical Modeling Study of Dopaminergic Retinal Neurons under Hyperpolarized Conditions

Takaaki Shirahata

Institute of Neuroscience and Kagawa School of Pharmaceutical Sciences, Tokushima Bunri University, Japan

Abstract A mathematical model of dopaminergic local circuit neurons isolated from the mouse retina (DA cells) was previously reported. This DA cell model was constructed based on the Hodgkin-Huxley formalism and is described by a system of nonlinear ordinary differential equations. The DA cell model contains four voltage-dependent ionic conductances: persistent sodium conductance, transient sodium conductance, fast potassium conductance, and slow potassium conductance. The present study involved a numerical simulation analysis of the DA cell model under hyperpolarized conditions to characterize these four ionic conductances. The analysis revealed a novel mechanism of repetitive spiking under hyperpolarized conditions. This mechanism contributes to the in-depth understanding of sodium conductances in DA cell models.

Keywords Mathematical Model, Numerical Simulation, Dopaminergic Neurons, Sodium Conductance

1. Introduction

Dopaminergic local circuit neurons isolated from the mouse retina (DA cells) can generate repetitive spiking when not hyperpolarized. A previous study developed a mathematical model based on the Hodgkin-Huxley formulation that reproduces this spiking behavior [1]. This DA cell model is described by a system of nonlinear ordinary differential equations (ODEs) and consists of four voltage-dependent ionic conductances: transient sodium conductance, persistent sodium conductance, fast potassium conductance, and slow potassium conductance. Previous studies also revealed that the DA cell model shows repetitive spiking behavior under certain hyperpolarized conditions [1, 2]. Although previous studies extensively investigated how variations in the above four ionic conductances affect the spiking behavior of the DA cell model under non-hyperpolarized conditions, hyperpolarized conditions have not been investigated in detail. A detailed analysis of ionic conductances is important [3]; thus, the effect of variations in ionic conductance on spiking behavior under hyperpolarized conditions was investigated using a computer simulation analysis of the DA cell model.

2. Materials and Methods

The present study investigated a previously described mathematical model of DA cells in the mouse retina [1]. The model is described by a system of six-coupled nonlinear ODEs, in which state variables are the membrane potential of the DA cells [V (mV)], and five gating variables of ionic currents (m_{NaT} , h_{NaT} , m_{NaP} , m_{KF} , and m_{KS}). The time evolution of the state variables is described as follows:

$$C_m \frac{dV}{dt} = I_{app} - I_{NaT}(V, m_{NaT}, h_{NaT}) - I_{NaP}(V, m_{NaP}) - I_{KF}(V, m_{KF}) - I_{KS}(V, m_{KS}) - I_L(V) \quad (1)$$

$$\frac{dm_{NaT}}{dt} = \frac{1}{\tau_{m_{NaT}}(V)} (m_{NaT,\infty}(V) - m_{NaT}) \quad (2)$$

$$\frac{dh_{NaT}}{dt} = \frac{1}{\tau_{h_{NaT}}(V)} (h_{NaT,\infty}(V) - h_{NaT}) \quad (3)$$

$$\frac{dm_{NaP}}{dt} = \frac{1}{\tau_{m_{NaP}}(V)} (m_{NaP,\infty}(V) - m_{NaP}) \quad (4)$$

$$\frac{dm_{KF}}{dt} = \frac{1}{\tau_{m_{KF}}(V)} (m_{KF,\infty}(V) - m_{KF}) \quad (5)$$

$$\frac{dm_{KS}}{dt} = \frac{1}{\tau_{m_{KS}}(V)} (m_{KS,\infty}(V) - m_{KS}) \quad (6)$$

where C_m ($= 8$ pF) is the membrane capacitance; I_{app} is the externally injected current of constant amplitude; I_{NaT}

* Corresponding author:

tshi@kph.bunri-u.ac.jp (Takaaki Shirahata)

Published online at <http://journal.sapub.org/ijtmp>

Copyright © 2017 Scientific & Academic Publishing. All Rights Reserved

(V , m_{NaT} , h_{NaT}), I_{NaP} (V , m_{NaP}), I_{KF} (V , m_{KF}), I_{KS} (V , m_{KS}), and I_L (V) are the transient sodium current, persistent sodium current, fast potassium current, slow potassium current, and leakage current, respectively, which are defined in Equations (7)–(11) below; $\tau_X(V)$ ($X = m_{NaT}$, h_{NaT} , m_{NaP} , m_{KF} , m_{KS}) and $Y(V)$ ($Y = m_{NaT,\infty}$, $h_{NaT,\infty}$, $m_{NaP,\infty}$, $m_{KF,\infty}$, $m_{KS,\infty}$) are the time constants of activation/inactivation and steady-state activation/inactivation functions, respectively, which are defined in Equations (12)–(21) below.

$$I_{NaT}(V, m_{NaT}, h_{NaT}) = g_{NaT} m_{NaT}^3 h_{NaT} (V - E_{Na}) \quad (7)$$

$$I_{NaP}(V, m_{NaP}) = g_{NaP} m_{NaP}^3 (V - E_{Na}) \quad (8)$$

$$I_{KF}(V, m_{KF}) = g_{KF} m_{KF}^4 (V - E_K) \quad (9)$$

$$I_{KS}(V, m_{KS}) = g_{KS} m_{KS}^4 (V - E_K) \quad (10)$$

$$I_L(V) = g_L (V - E_L) \quad (11)$$

$$\tau_{m_{NaT}}(V) = 0.31 + \frac{0.79 - 0.31}{1 + e^{(V+24)/4.9}} \quad (12)$$

$$\tau_{h_{NaT}}(V) = 0.51 + \frac{3.35 - 0.51}{1 + e^{(V+40)/10.5}} \quad (13)$$

$$\tau_{m_{NaP}}(V) = 0.25 \quad (14)$$

$$\tau_{m_{KF}}(V) = 1.6 + \frac{7.8 - 1.6}{1 + e^{(V+16.6)/2.3}} \quad (15)$$

$$\tau_{m_{KS}}(V) = 6.3 + \frac{15.4 - 6.3}{(1 + e^{(V-10.9)/11.6})(1 + e^{-(V-11.4)/9.5})} \quad (16)$$

$$m_{NaT,\infty}(V) = \frac{1}{1 + e^{-(V+47)/7.3}} \quad (17)$$

$$h_{NaT,\infty}(V) = \frac{1}{1 + e^{(V+77)/7.3}} \quad (18)$$

$$m_{NaP,\infty}(V) = \frac{1}{1 + e^{-(V+34)/13.7}} \quad (19)$$

$$m_{KF,\infty}(V) = \frac{1}{1 + e^{-(V+23.6)/26.8}} \quad (20)$$

$$m_{KS,\infty}(V) = \frac{1}{1 + e^{-(V+22)/17.1}} \quad (21)$$

where g_{NaT} , g_{NaP} , g_{KF} , g_{KS} , and g_L ($= 0.4$ nS) are the maximal conductances of I_{NaT} (V , m_{NaT} , h_{NaT}), I_{NaP} (V , m_{NaP}), I_{KF} (V , m_{KF}), I_{KS} (V , m_{KS}), and I_L (V), respectively; E_{Na} ($= 80$ mV), E_K ($= -80$ mV), and E_L ($= -50$ mV) are the reversal potentials of sodium currents [I_{NaT} (V , m_{NaT} , h_{NaT}) and I_{NaP} (V , m_{NaP})], potassium currents [I_{KF} (V , m_{KF}) and I_{KS} (V , m_{KS})], and I_L (V), respectively. Refer to [1] for detailed explanations of the Equations (1)–(21).

The free and open source software Scilab (<http://www.scilab.org/>) was used to numerically solve the above Equations (1)–(21) (initial conditions: $V = -70$ mV, $m_{NaT} = 0.05$, $h_{NaT} = 0.32$, $m_{NaP} = 0.05$, $m_{KF} = 0.2$, and $m_{KS} = 0.08$). The total simulation time was 2.5 s for all simulations. The system parameters whose values were varied were I_{app} , g_{NaT} , g_{NaP} , g_{KF} , and g_{KS} . To make the DA cell model hyperpolarized, I_{app} was varied from -9 to -7 pA at an interval of -1 pA. In previous studies [1, 2], the DA cell model was hyperpolarized by increasing the g_L value. However, the present study simulated hyperpolarized conditions by changing the I_{app} value because this value can be easily regulated in electrophysiological experiments. The default values of g_{NaT} , g_{NaP} , g_{KF} , and g_{KS} were 270 nS, 6.7 nS, 47 nS, and 9.5 nS, respectively. To evaluate the effect of variations in ionic conductances on the DA cell model, the g_{NaT} , g_{NaP} , g_{KF} , and g_{KS} were each varied from 0 to 200% of each default value at an interval of 20%.

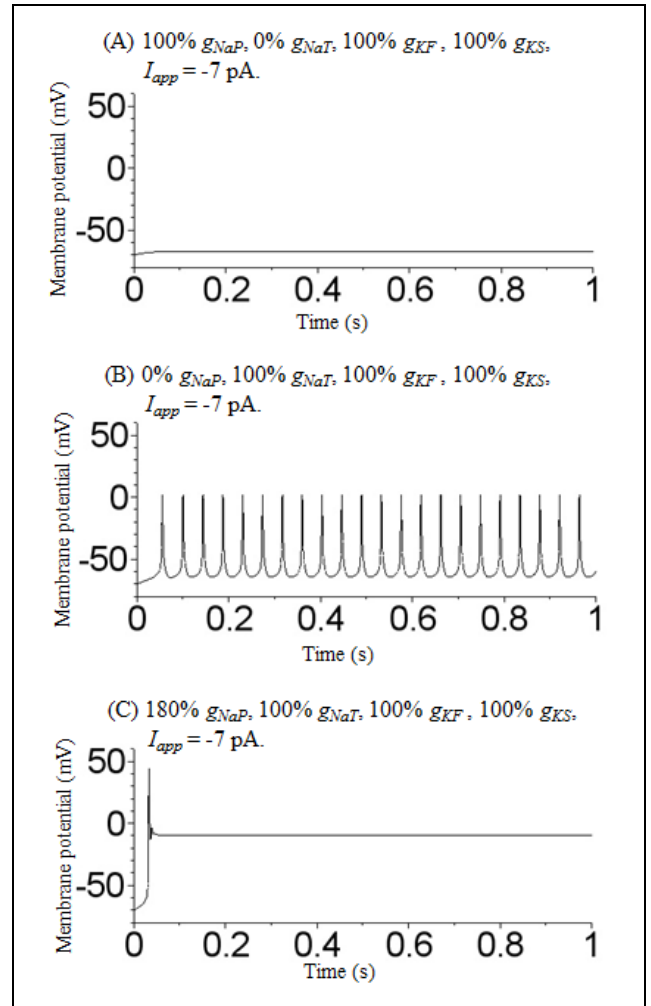


Figure 1. Time courses of the membrane potential of a model of DA cells in the mouse retina under conditions of (A) 100% g_{NaP} , 0% g_{NaT} , 100% g_{KF} , 100% g_{KS} , and $I_{app} = -7$ pA; (B) 0% g_{NaP} , 100% g_{NaT} , 100% g_{KF} , 100% g_{KS} , and $I_{app} = -7$ pA; and (C) 180% g_{NaP} , 100% g_{NaT} , 100% g_{KF} , 100% g_{KS} , and $I_{app} = -7$ pA

3. Results

By varying I_{app} , g_{NaP} , g_{NaT} , g_{KF} , and g_{KS} in the DA cell model, we found three dynamic states. The first was a hyperpolarized steady-state. An example of the time course of the membrane potential of the DA cell model in this state is shown in Figure 1A. The membrane potential in this state is stabilized at a value below -50 mV. The second is a repetitive spiking state. An example of the time course of the

membrane potential in this state is shown in Figure 1B. Oscillatory activity of the membrane potential was observed in this state. The third is a depolarized steady-state. An example of the time course of the membrane potential in this state is shown in Figure 1C. This state is similar to a hyperpolarized state in that it was also stabilized at a specific value. However, in contrast to Figure 1A, the value of the membrane potential was stabilized at a more positive potential (i.e., a value above -10 mV).

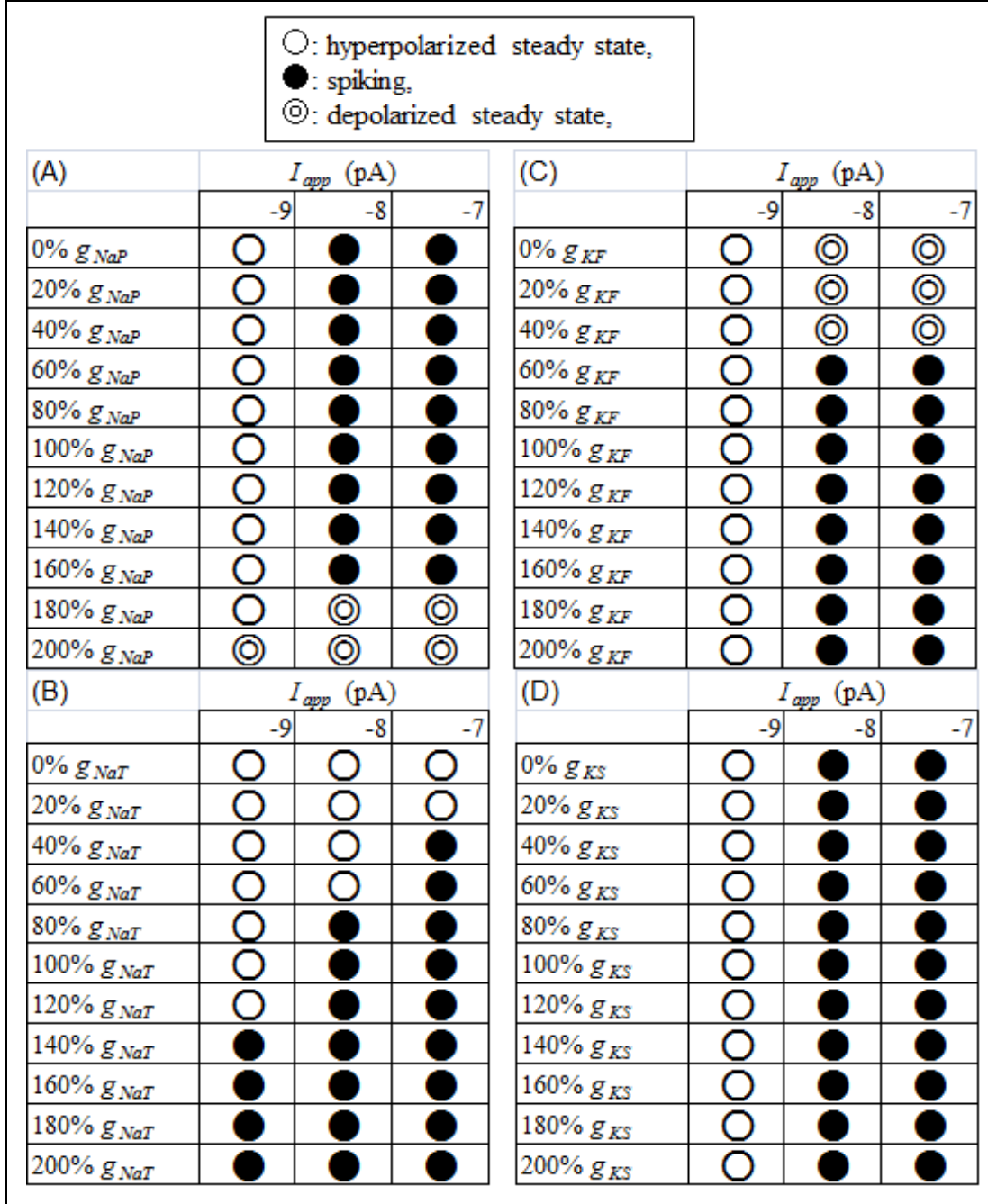


Figure 2. The dependence of the dynamic states of DA cells in the mouse retina on (A) I_{app} and g_{NaP} , (B) I_{app} and g_{NaT} , (C) I_{app} and g_{KF} , and (D) I_{app} and g_{KS} . ○ indicates a hyperpolarized steady-state; ● indicates a repetitive spiking state; ⊙ indicates a depolarized steady-state

The dependence of the above three dynamic states on I_{app} and ionic conductance values were revealed in detail (Figure 2). The present study investigated the dynamic states in the (I_{app}, g_{NaP}) parameter space (Figure 2A), (I_{app}, g_{NaT}) parameter space (Figure 2B), (I_{app}, g_{KF}) parameter space (Figure 2C), and (I_{app}, g_{KS}) parameter space (Figure 2D). In the (I_{app}, g_{NaP}) parameter space (Figure 2A), a hyperpolarized steady-state appeared when I_{app} was -9 pA under conditions in which g_{NaP} was between 0% and 180% of a default value. A repetitive spiking state appeared when I_{app} was between -8 pA and -7 pA under conditions in which g_{NaP} was between 0% and 160% of a default value. A depolarized steady-state appeared when 1) I_{app} was -9 pA and g_{NaP} was 200% of a default value and 2) I_{app} was between -8 pA and -7 pA under conditions in which g_{NaP} was 180% and 200% of a default value. In the (I_{app}, g_{NaT}) parameter space (Figure 2B), only two dynamic states (i.e., a hyperpolarized steady-state and a repetitive spiking state) appeared. An increase in g_{NaT} at each I_{app} value changed the dynamic state from a hyperpolarized steady-state to a repetitive spiking state. In addition, a decrease in the I_{app} value induced an increase in the g_{NaT} threshold for the transition from a hyperpolarized steady-state to a repetitive spiking state. In the (I_{app}, g_{KF}) parameter space (Figure 2C), a hyperpolarized steady-state appeared when I_{app} was -9 pA irrespective of the g_{KF} value. A repetitive spiking state appeared when I_{app} was between -8 pA and -7 pA under conditions in which g_{KF} was between 60% and 200% of a default value. A depolarized steady-state appeared when I_{app} was between -8 pA and -7 pA under conditions in which g_{KF} was between 0% and 40% of a default value. In the (I_{app}, g_{KS}) parameter space (Figure 2D), only two dynamic states (i.e., a hyperpolarized steady-state and a repetitive spiking state) appeared. A hyperpolarized steady-state appeared when I_{app} was -9 pA irrespective of the g_{KS} value. A repetitive spiking state appeared when I_{app} was -8 and -7 pA irrespective of the g_{KS} value.

4. Discussions

The present study performed a numerical simulation of a DA cell model and detailed the dependence of the dynamic states of the model under hyperpolarized conditions on four ionic conductances (i.e., g_{NaT} , g_{NaP} , g_{KF} , and g_{KS}). Previous studies showed that repetitive spiking of the DA cell model under hyperpolarized conditions stops in the absence of either g_{NaT} or g_{NaP} [1, 2]. However, the effect of increases in g_{NaT} and g_{NaP} and variations in g_{KF} and g_{KS} on the DA cell model under hyperpolarized conditions remained unclear. To resolve this problem, the present study systematically investigated the effect of both an increase and decrease in all four ionic conductances and revealed previously unreported methods for preventing repetitive spiking under hyperpolarized conditions: an increase in g_{NaP} (Figure 2A) and a decrease in g_{KF} (Figure 2C). In addition, the finding that the absence of g_{NaT} stops repetitive spiking under hyperpolarized conditions (Figure 1A and Figure 2B) is

consistent with previous studies [1, 2]. Interestingly, although the previous result indicated that repetitive spiking under hyperpolarized conditions stops in the absence of g_{NaP} [2], the present study cannot reproduce this result (Figure 1B and Figure 2A). Although both the previous [2] and present studies investigated the DA cell model under hyperpolarized conditions, these conditions were implemented differently. The previous study hyperpolarized the model by increasing a leak conductance, whereas the present study hyperpolarized the model by externally injecting a negative current. Based on this difference, the present study cannot completely reproduce the previous result. In summary, we can categorize the mechanism underlying repetitive spiking of the DA cell model under hyperpolarized conditions into two types: (1) under one hyperpolarized condition, both the transient and persistent sodium conductances are necessary for repetitive spiking, and neither the transient sodium conductance alone nor the persistent sodium conductance alone is sufficient for repetitive spiking [2] and (2) under another hyperpolarized condition, only the transient sodium conductance is necessary and sufficient for repetitive spiking, and the persistent sodium conductance is not required for repetitive spiking (Figure 2A and 2B). Type (2) is a novel mechanism discovered in the present study.

Although the present study investigated the dependence of the dynamic states of the DA cell model on various ionic conductances, similar findings have been reported in other neuron models [4-6]. These three studies focused on dynamic states under depolarized conditions, whereas the present study focused on the dynamic states under hyperpolarized conditions. Similar to the DA cell model, a medial vestibular nucleus neuron (mVNN) model can generate repetitive spiking [7]. In addition, the dependence of the dynamic states of the mVNN model under hyperpolarized conditions on ionic conductances was also reported [8]. This previous study revealed the relationship between two dynamic states (i.e., a repetitive spiking state and a hyperpolarized steady-state) and ionic conductances [8]. However, the present study revealed the relationship between three dynamic states (i.e., a repetitive spiking state, a hyperpolarized steady-state, and a depolarized steady-state) and ionic conductances.

5. Conclusions

The present study completed a numerical simulation of the DA cell model under hyperpolarized conditions and characterized four voltage-dependent ionic conductances. The importance of the present study is that it identified a novel mechanism of repetitive spiking: repetitive spiking under certain hyperpolarized conditions depends on the transient sodium conductance but not on the persistent sodium conductance. This contributes to a deeper understanding of sodium conductance characteristics in the DA cell model.

ACKNOWLEDGEMENTS

The author would like to thank Enago (www.enago.jp) for the English language review.

REFERENCES

- [1] Steffen, M. A., Seay, C. A., Amini, B., Cai, Y., Feigenspan, A., Baxter, D. A., Marshak, D. W. (2003) Spontaneous activity of dopaminergic retinal neurons. *Biophysical Journal*, 85, 2158-2169.
- [2] Shirahata, T. (2011) The effect of variations in sodium conductances on pacemaking in a dopaminergic retinal neuron model. *Acta Biologica Hungarica*, 62, 211-214.
- [3] Ashrafuzzaman, M. and Tuszynski, J. (2012) *Membrane Biophysics*, p. 26, Heidelberg, Springer.
- [4] Golomb, D. (2014) Mechanism and function of mixed-mode oscillations in vibrissa motoneurons. *PLoS ONE*, 9, e109205. doi:10.1371/journal.pone.0109205.
- [5] Shirahata, T. (2016) The relationship of sodium and potassium conductances with dynamic states of a mathematical model of electrosensory pyramidal neurons. *Applied Mathematics*, 7, 819-823.
- [6] Shirahata, T. (2016) The effect of variations in ionic conductance values on the dynamics of a mathematical model of nonspiking A-type horizontal cells in the rabbit retina. *Applied Mathematics*, 7, 1297-1302.
- [7] Av-Ron, E. and Vidal, P.P. (1999) Intrinsic membrane properties and dynamics of medial vestibular neurons: a simulation. *Biological Cybernetics*, 80, 383-392.
- [8] Shirahata, T. (2016) The effect of variations in ionic conductance values on the suppression of repetitive spiking in a mathematical model of type-A medial vestibular nucleus neurons. *Applied Mathematics*, 7, 1134-1139.